Hydrol. Earth Syst. Sci. Discuss., 9, 11733–11768, 2012
www.hydrol-earth-syst-sci-discuss.net/9/11733/2012/
doi:10.5194/hessd-9-11733-2012

Hydrology and Earth System Sciences Discussions

Linking ENSO and heavy rainfall events over Coastal British Columbia through a weather pattern classification

P. Brigode*[1,2], Z. Mićović[3], P. Bernardara[1], E. Paquet[4], F. Garavaglia[4], J. Gailhard[4], and P. Ribstein[2]

[1]LNHE, R&D, Electricité de France, Chatou, France
[2]UMR 7619 Sisyphe, Université Pierre et Marie Curie, Paris, France
[3]BC Hydro, Engineering, Burnaby, BC, Canada
[4]DTG, DMM, Electricité de France, Grenoble, France
[*]*Invited contribution by P. Brigode, one of the EGU, Union Outstanding Student Poster (OSP) Award winners 2012.*

Received: 6 September 2012 – Accepted: 9 October 2012 – Published: 15 October 2012

Correspondence to: P. Brigode (pierre.brigode@edf.fr)

Published by Copernicus Publications on behalf of the European Geosciences Union.

Linking ENSO and heavy rainfall events over Coastal British Columbia

P. Brigode et al.

Abstract

Classifications of atmospheric weather patterns (WPs) are widely used for the description of the climate of a given region and are employed for many applications, such as weather forecasting, downscaling of global circulation model outputs and reconstruction of past climates. WP classifications were recently used to improve the statistical characterisation of heavy rainfall. In this context, bottom-up approaches, combining spatial distribution of heavy rainfall observations and geopotential height fields have been used to define WP classifications relevant for heavy rainfall statistical analysis. The definition of WPs at the synoptic scale creates an interesting variable which could be used as a link between the global scale of climate signals and the local scale of precipitation station measurements. We introduce here a new WP classification centred on the British Columbia Coastal region (Canada) and based on a bottom-up approach. Five contrasted WPs composed this classification, four rainy WPs and one non-rainy WP, the anticyclonic pattern. The four rainy WPs are mainly observed in the winter months (October to March), which is the period of heavy precipitation events in Coastal BC and is thus consistent with the local climatology. The combination of this WP classification with the seasonal description of rainfall is shown to be useful for splitting observed precipitation series into more homogeneous sub-samples and thus identifying, for each station, the synoptic situations that generate the highest hazard in terms of heavy rainfall events. El Niño Southern Oscillations significantly influence the frequency of occurrence of two Coastal BC WPs. Within each WP, ENSO seem to influence only the frequency of rainy events and not the magnitudes of heavy rainfall events. Consequently, MEWP heavy rainfall estimations do not show significant evolution of heavy rainfall behaviour between Niño and Niña winters. However, the WP approach captures the variability of the probability of occurrences of synoptic situations generating heavy rainfall depending on ENSO and opening interesting perspectives for the analysis of heavy rainfall distribution in a non-stationary context.

HESSD

9, 11733–11768, 2012

1 Introduction

Traditionally in the framework of the extreme value theory, the probability of extreme rainfall is estimated by fitting an extreme value distribution over a sample of rainfall observation series at a given location (Fréchet, 1927; Gumbel, 1958; Pickands, 1975; Coles et al., 2003). This approach assumes (strongly) that the sample used is independent, stationary and homogeneous. However, the heaviest rainfall events can have various atmospheric geneses (convective rainfall and frontal rainfall, for example) and they show generally strong seasonal variability (Djerboua and Lang, 2007). In a recent study, Allamano et al. (2011) showed the significant bias induced by neglecting the seasonality of hydrological extremes in determining extreme value probabilities. In this general framework, Garavaglia et al. (2010, 2011) proposed a multi-exponential weather pattern (MEWP) probability distribution for extreme rainfall based on a weather pattern (WP) and seasonal sub-sampling. Other authors recently used the WP concept to characterise extreme rainfall events (e.g. Ducić et al., 2012). More generally, since early WP classifications such as the subjective classification produced by Pague and Blandford (1897) over the Northwestern US, the definition of WP classification at the synoptic scale has been shown to be useful for the estimation of statistical characteristics of hydroclimatic records such as precipitation or streamflow series at the local scale. Moreover, WP frequency of occurrence has been linked to global signals such as North Atlantic Oscillation (NAO) or El Niño Southern Oscillations (ENSOs). For example, Fernández-González et al. (2011) investigated the dependence between NAO frequencies and Spanish WPs. Several studies showed the significant correlation between WP frequency and ENSO climate signals over Northwestern America (Kimoto and Ghil, 1993; Chen and van den Dool, 1999; Robertson and Ghil, 1999; Sheridan, 2002; Stahl et al., 2006) or even over Louisiana (McCabe and Muller, 2002). Consequently, the link between global signals and hydroclimatic variables, which is investigated for instance by Fernández-González et al. (2011) and Schubert et al. (2008), can be explored through a WP classification approach. Casola and Wallace (2007) found

HESSD
9, 11733–11768, 2012

significant correlations between ENSOs and the frequency of occurence of the four winter WPs they previously identified using a limited-contour clustering algorithm to the pentad (5-day average) 500 hPa geopotential height field data for the Pacific–North American region. They also showed the existing link between frequency of occurence of extreme weather (coldest and wettest winter days) and the frequency of occurence of WPs, highlighting that this signal is much weaker for precipitation than for temperature extreme events. In conclusion and explaining the limits of the methodology used, they stated that "with the exception of the Pacific Northwest, the clustering method performs poorly in segregating incidences of extreme precipitation. We speculate that precipitation is inherently dependent on synoptic scale events that are associated with patterns smaller in spatial scale and shorter in time scale than the patterns captured here."

In this framework, the Coastal region of British Columbia (BC) represents a very interesting playground, since numerous authors have studied the links between the rainfall probability distribution over the Pacific Coast of North America and some large-scale climatological phenomena, such as ENSOs, the Pacific Decadal Oscillation (PDO) or the Pacific North America pattern (PNA). These oscillations are linked to both average winter rainy events (Yarnal and Diaz, 1986; Shabbar et al., 1997) and winter extreme events (Gershunov, 1998; Cayan et al., 1999) all over the North Pacific Coast. Concerning extreme rainfall, Higgins et al. (2000) pointed out the highest frequency of heavy rainfall events during the neutral years preceding warm ENSO winters. However, Kenyon and Hegerl (2010) did not find a clear, significant difference between El Niño winter extremes (defined as the largest amount of daily precipitation over a single day and over 5 days) and other winters over BC. In a recent study on the influences of climate mode variability on global extreme precipitation, Feldl and Roe (2011) showed that warm phases of ENSOs implied both changes of mean precipitation and precipitation distribution shapes over the American West. Zhang et al. (2010) also noted the clear influence of ENSOs and PDO on daily winter extreme precipitation values over North America, but with an unclear signal over BC, a region that is poorly studied due to a limited number of available data. Finally, Mass et al. (2011) mentioned natural variability as a possible explanation for the low increasing trend of extreme precipitation found over the Pacific Coast. Studying the genesis of Northern Washington floods, Neiman et al. (2011) showed that most floods are produced by "atmospheric river" (AR) situations, which are relatively narrow regions of the atmosphere that are responsible for most of the horizontal transport of water vapor outside of the tropics (the "Pineapple Express" is a well-known example of a strong AR that brings moisture from the Hawaiian tropics region to the North American west coast Dettinger, 2004). In AR situations over North-Western Washington, they showed that floods are observed on several watersheds depending on the orientation of the AR and the elevation distribution over the watershed areas. These results suggest some correlations between climate signals and rainfall behaviour over the Coastal region of BC. Even so, scientific questions on the nature of the correlations remain open. The WP classification appears thus to be a "medium-scale disaggregating tool" between climate signals and local rainfall observations and it deserves to be tested in this context.

The aim of this paper is thus to define a WP classification based on a bottom-up approach introduced by Garavaglia et al. (2010), which is useful for heavy rainfall analysis of the Coastal BC region and to use the WP approach to study the links between ENSOs and BC heavy rainfall events. The method used for the WP classification and heavy rainfall analysis is summarised in Sect. 2. The rainfall and geopotential data sets used in the study are described in Sect. 3, while Sect. 4 presents and discusses the results obtained. Finally, Sect. 5 draws conclusions.

2 Methodology

2.1 Bottom-up approach for the definition of a weather pattern classification

WPs are identified using a "bottom-up" approach: firstly identifying rainfield patterns using rainfall information ("bottom" step) and secondly projecting them into a geopotential height space for the final definition of WP ("up" step). The methodology which is described and used in Garavaglia et al. (2010) for the definition of eight French WPs and in Brigode et al. (2012) for the definition of five Austrian WPs, is summarised in the following four stages.

2.1.1 Selection of a rainy day population

A sub-sample of the heaviest daily precipitations is selected using a spatial averaging criterion, whereby for each day in the record, the daily average precipitation of all stations is calculated. The top 20 % days are selected as "rainy days" in this study. For a 20-yr record period, this 20 % threshold selects 1524 rainy days. The other 6136 days are at this stage combined in a non-rainy class. The need for a classification more closely focussed on "where it rains" than on "how much it rains" (i.e. having classes regrouping days that are particularly rainy in the same area rather than having classes regrouping days with the same amount of rain) is fulfilled by using the "shapes" of the daily rainfall fields. For each day, a rainfall shape field is estimated by normalising the daily precipitation observed at each station by the average precipitation observed over the entire region of interest.

2.1.2 Hierarchical Ascendant Classification of the rainy day "shapes" fields

A Hierarchical Ascendant Classification (HAC) is then performed on the rainy day "shapes" fields previously identified. The rainy classes are generated using the Ward method (1963), which iteratively chooses the grouping presenting the minimum intra-class inertia (Cheng and Wallace, 1993). The final number of rainfall classes is determined by first examining numerical criteria such as changes in intra-class inertia as a function of the number of classes and second by looking at the spatial distribution of each rainfall class in the selected area. This choice is thus a mixture of numerical criteria analysis and climatological assessment.

Discussion Paper | Discussion Paper | Discussion Paper | Discussion Paper |

HESSD

9, 11733–11768, 2012

Linking ENSO and heavy rainfall events over Coastal British Columbia

P. Brigode et al.

2.1.3 Projection of the rainy classes into one geopotential height field space

The daily synoptic situation over the area of interest is described using gridded geopotential height fields at two pressure levels (700 hPa and 1000 hPa), twice a day (at 0 h and 24 h, allowing a dynamical description of the geopotential height fields over 24 h). Thus, each day (d) is characterised by two couples of geopotential height fields: the first couple is composed of a 700 hPa geopotential field at 0 h and a 700 hPa geopotential at 24 h (equivalent to the 700 hPa geopotential field of the day ($d+1$) at 0 h) and the second couple is composed of a 1000 hPa geopotential field at 0 h and a 1000 hPa geopotential field at 24 h (equivalent to the 1000 hPa geopotential field of the day ($d+1$) at 0 h). These options are the results of previous studies on quantitative precipitation forecasting using the analogue method in France (Guilbaud and Obled, 1998; Obled et al., 2002; Bontron, 2004). The 1000 hPa fields are strongly correlated to the rainfall ones since they describe the pressure situation on the ground and catch the local patterns, while the 700 hPa fields give information at a larger scale and catch the synoptic systems and movements. The geopotential space used for the French WP classification (Garavaglia et al., 2010) and the Austrian WP classification (Brigode et al., 2012) was composed of these four geopotential fields defined, respectively, on 110 grid points centred on South-Eastern France and on 54 grid points centred on the Western Alps. Defining the geopotential height space that gives robust information for explaining the rainfall-generating processes coming from the synoptic scale is the critical point of these “up” steps. Once one geopotential space is defined, the centroids of the rainy classes and of the non-rainy class previously identified are calculated in this space, by estimating the four average geopotential fields of the days composing each rainy class. Finally, each class centroid is characterised by two couples of geopotential height fields (700 hPa at 0 h, 1000 hPa at 0 h, 700 at 24 h and 1000 hPa at 24 h).

HESSD
9, 11733–11768, 2012

2.1.4 Re-assignment of each day to a weather pattern

The last classification step consists in the re-assignment of each day (considered as rainy or non-rainy) to a given WP in estimating Teweles and Wobus (1954) distances between the day considered and all the class centroids. The need to focus on the field shapes is the main criterion for choosing this distance, which considers the synoptic circulation gradients (Obled et al., 2002). The final Teweles-Wobus distance between one particular day and one class centroid is defined as the sum of the four distances between the four geopotential height fields (700 and 1000 hPa at 0 h and 700 and 1000 hPa at 24 h) of the day considered and of the centroid considered.

2.2 Multi-exponential weather pattern distributions

MEWP distributions are estimated for each rainfall series following the approach introduced by Garavaglia et al. (2010). Note that MEWP distributions are fitted on a sample of "centred rainy events" over a threshold, noted CR hereafter. The CR population is defined as days having higher precipitation values than the previous and following days. Using this sub-sampling allows working on a distribution of (so-considered) independent events, which is much more dense than annual maximums for example. Moreover, note that seasonal MEWPs are defined, where seasons generally consist in grouping three or four continuous months of similar rainfall hazard values. In BC, the rainy season is mainly constituted by the winter months both for the common and the heaviest events. Heavy rainfall analysis has thus been limited in this study to a critical season of 6 winter months, from October to March. This "long" winter season allows working on relatively long rainfall sub-populations. Formulation of MEWP distribution is reported in the following:

HESSD
9, 11733–11768, 2012

$$F^i(\mathrm{CR}) = \sum_{j=1}^{n_{\mathrm{WP}}} F^i_j(\mathrm{CR}) \cdot p^i_j$$
$$F^i(\mathrm{CR}) = \sum_{j=1}^{n_{\mathrm{WP}}} \left[1 - \exp\left(-\frac{\mathrm{CR} - u^i_j}{\lambda^i_j}\right)\right] \cdot p^i_j \quad (1)$$

where i is the season studied, CR are the central rainfall event observations, j is the WP studied, n_{WP} is the number of WPs, p is the CR event probability of occurrence of the WP, F is the marginal distribution, u is the threshold for heavy rainfall observation selection and λ is the parameter of the exponential law. Thus, the MEWP distribution defined on a given rainfall series is characterised by two parameters per WP and per season (scale parameter λ (called Gradex and values in mm/24 h) and threshold parameter u – values in mm) and one extra parameter per WP and per season, which is the frequency of occurrences of the WP CR observations (parameter p). The following expression gives the relation between MEWP probability and return period, in years:

$$T(\mathrm{CR}) = \frac{1}{1 - F(\mathrm{CR})^{\frac{n}{N}}} \quad (2)$$

where n is the size of the rainfall observation sample considered (for example, the number of winter CR events of WP1) and N is the number of years of the CR series considered.

2.3 Influence of ENSO on WP frequency and on MEWP parameters and distributions

Each observed winter (ONDJFM) will firstly be characterised as "Niño winter", "neutral winter" or "Niña winter", according to SST Niño 3.4 index (Trenberth, 1997), described in Sect. 3.3. Three winter sub-sets will thus be defined (Niño, neutral and Niña winters).

HESSD
9, 11733–11768, 2012

The frequency of each WP is then estimated on the Niño and the Niña winter sub-sets. Bootstrap simulations are then performed in order to test the significance of the frequency difference between the Niño and the Niña winter sub-sets. For a given period, 1000 random winter combinations are generated among all the winters available over the period considered. Each of the 1000 random winter combinations is composed by the same number of winters, which is equal to half of the total number of winter of the period considered, i.e. for a given period composed of 20 winters, 1000 combinations of 10 winters will be constructed. Note that the bootstrap simulation performed does not allow having a particular winter more than once in one combination of winters. WP frequency will be finally estimated on each of the 1000 combinations generated, in order to quantify the natural variability of WP frequency and thus to compare the frequency estimated on particular ENSO sub-sets compared to all the sub-sets (without consideration for ENSOs) generated by bootstrap simulations. Note that a similar methodology has been applied by Casola and Wallace (2007) for identifying the correlation between ENSO and the frequency of occurrence of four Pacific–North American winter WPs. After discussing the influence of ENSOs on Coastal BC WP frequency, more local tests will be performed to determine the influence of ENSO on rainfall characteristics over several Coastal BC rainfall stations. MEWP parameters will first be identified over each rainfall station considered and over all the available winters. These parameters (three per station) will then be compared with the MEWP parameters obtained over the same stations but over two different winter sub-sets, the Niño and the Niña winter sub-sets. Final heavy rainfall MEWP estimations will be compared with the 1000-yr return period precipitation values for each station identified over the different winter sub-sets. The significance of potential parameter changes between the different sub-sets will also be tested with bootstrap simulations. The bootstrap methodology is the same as the one used for testing the influence of ENSOs on Coastal BC WP frequency: MEWP parameters will be defined for each station on 1000 random winter combinations, in order to quantify the natural variability of the different parameters studied and thus to compare

HESSD
9, 11733–11768, 2012

the parameters estimated on particular ENSO subsets with all the subsets generated by bootstrap simulations.

3 Data

3.1 Data sets used for WP definition

WPs have been defined combining both rainfall information, captured by daily precipitation series, and synoptic information, captured by daily geopotential height reanalysis. A total of 177 stations were selected for the definition of Coastal BC rainfall classes in order to have a good representation of local climatology and potential local rainy patterns. Daily precipitation data is available on each of the 177 stations for the 1983–2003 period, allowing the definition of rainfall classes for this 20-yr period. Note that the stations used are located in the Coastal BC region (Canada) and also in Western Washington (USA). In the following, this region will be called Coastal BC. The data quality has been checked, looking for statistically abnormal trends for each series compared to the nearest ones and looking for aberrant data. Location of the rainfall stations is reported in Fig. 1a with blue dots.

The geopotential height fields, provided by the Twentieth Century Reanalysis Project data set (Compo et al., 2011) from the National Oceanic and Atmospheric Administration (NOAA) are defined on a 2-degree resolution grid from 1871 to 2008 for both 700 and 1000 hPa. The geopotential space was chosen and is defined on 338 points centered on the Washington State coast, from −150° W to −100° W and from 36° N to 60° N. This assessment was made looking at several historical storm synoptic situations: the geopotential space size and position has to be defined in order to catch these storm systems, which mainly come from the Pacific Ocean, but also from inland systems. Spatial coverage of the 338-point grid is shown on Fig. 1b with black dots. Note that using both 500 hPa and 1000 hPa (instead of using 700 hPa and 1000 hPa) fields was also tested, showing no major differences in terms of the patterns identified. Thus, the

HESSD
9, 11733–11768, 2012

geopotential space further used is made up of four fields of 338 points for each day: 700 and 1000 hPa at 0 h and 700 and 1000 hPa at 24 h. The geopotential height data set was first extracted over the 1983–2003 period, which is the time period covered by the rainfall data set. In the second step, the entire available geopotential height data set (1871–2008) was used, extending the WP classification defined on the 1983–2003 period over a longer period.

3.2 Rainfall series used for the quantification of ENSO influence on rainfall characteristics

Long precipitation records are needed when impacts of climate signals such as ENSO on rainfall are studied. Forty-five stations with 50 yr of data (from 1951 to 2001) were selected. The position of the stations is shown in Fig. 1a with red dots. Note that these stations are mainly in low-elevation areas and are included in the rainfall data sets used for the definition of weather patterns. The influence of ENSO on rainfall characteristics will thus be assessed over this 50-yr period, starting in 1951 and finishing in 2001.

3.3 Data set used for ENSO classification

El Niño Southern Oscillations are further described with the SST Niño 3.4 Index, which consists in monthly sea surface temperature (SST) anomalies in degrees Celsius estimated on the 3.4 Niño region, bounded by 120° W–170° W and 5° S–5° N (Trenberth, 1997). A classification of ENSO winters has been defined using this data set: each winter (ONDJFM) is characterised by an average monthly SST anomaly estimated on the December, January and February months. Winters with SST anomalies below −0.5 °C are considered as La Niña winters, winters with SST anomalies above −0.5 °C and below 0.4 °C are considered as neutral winters and winters with SST anomalies above 0.4 °C are considered as El Niño winters. The ENSO winter classification is illustrated on Fig. 2, showing that 53 Niño winters and 48 Niña winters are identified over the 1872–2007 period (the first period used for the quantification of the influence of

Discussion Paper | Discussion Paper | Discussion Paper | Discussion Paper |

HESSD

9, 11733–11768, 2012

Linking ENSO and heavy rainfall events over Coastal British Columbia

P. Brigode et al.

ENSO on WP frequency) and that 20 Niño winters and 17 Niña winters are identified on the 1951–2001 period (the second period used for the quantification of the influence of ENSO on WP frequency and the period used for quantification of the influence of ENSO on rainfall characteristics).

4 Results

4.1 Empirical evidence of the relation between ENSOs and Coastal BC rainfall distribution

Empirical evidence on the correlation between Coastal BC rainfall distribution and ENSO are investigated first.

For each of the 45 stations considered, Fig. 3 presents the relative differences between rainfall characteristics of all the record periods (50 winters) and over the Niña winters (17 winters) and the relative differences between rainfall characteristics of the all record periods (50 winters) and over the Niño winters (20 winters). Four characteristics were estimated: (a) the average of winter precipitation values, (b) the frequency of the days when more than 20 mm were observed, (c) the 0.70 percentile and (d) the 0.95 percentile of the rainfall distributions. The blue and red histogramms represent for each of the four graphs the distributions of the (x) and the (y) axis values. Significant differences are observed in terms of average winter amount of rain over Coastal BC, with about 8 % more rain during Niña winters compared to all winters, and −8 % rain during Niño winters compared to all winters. The difference between Niño and Niña winters is less significant in terms of frequency of heavy rainy days (here days with 20 mm or more observed). Finally, heavy (percentile 0.70) and extreme quantiles (percentile 0.95) also show an unclear signal, with percentile values slightly lower during Niño winters and slightly higher during Niña winters, especially for the heavy rainfall event percentile.

HESSD
9, 11733–11768, 2012

4.2 Coastal BC WP definition for heavy rainfall analysis

In this section, the Coastal BC WPs are presented in terms of geopotential height anomaly fields, spatial precipitation fields and monthly frequency of occurence.

Figure 4a shows the geopotential height anomaly fields (1000 hPa at 0 h) and 4b the station ratio between the mean precipitation amount and the general precipitation amount (considering all WPs) for each of the five Coastal BC WPs. Finally, Fig. 4c presents the monthly frequency of each WP. WP1 (9 % of all days) groups rainy days throughout the Coastal BC region. WP2 (15 % of all days) is characterised by almost North-South circulation which engendered particularly rainy events in the Washington State stations and Vancouver City area. WP3 (17 % of all days) groups days with more South-Western–North-Eastern circulations, which bring a lot of rain in the central part of the Vancouver Island region. WP4 (27 % of all days) is characterised by the same oriented circulations but with a northern latitudinal translation and thus rainy days in the northern part of the Coastal BC region. Finally, the non-rainy pattern WP5 (32 % of all days) comprises typical anticyclonic situations, with essentially non-rainy days.

Table 1 summarises yearly and seasonal frequencies of the five Coastal BC WPs for the 1871–2003, 1951–2001 and 1983–2003 periods. The WP frequencies exhibit a clear seasonal signal, with rainy patterns (WP1 to WP4) occurring mainly in the winter months, while summer months are characterised mostly by the anticyclonic pattern WP5 (more than 50 % of summer days are assigned to anticyclonic weather pattern). WP frequencies seem to be relatively stationary over time since frequencies over the 1983–2003 period (20-yr period used for the definition of the WP centroids) are equivalent to frequencies over the 1871–2007 period.

4.3 MEWP parameters and distributions

In this section, a spatial analysis of the Gradex values (λ parameters of Eq. 1) obtained over 45 rainfall stations and an example of a MEWP distribution are illustrated.

HESSD
9, 11733–11768, 2012

Figure 5a shows ratios estimated for each rainfall station and each WP between the Gradex value of the WP considered and the average value of the five Gradex values for the station considered. One particular station (McMillin reservoir, Washington State) is highlighted on this map since it will be used as an example of the construction of a MEWP distribution. Thus, Fig. 5b shows for each WP a comparison between the whole CR distribution of the McMillin reservoir rainfall series and CR sub-samples of the WP considered. Finally, Fig. 5c presents the final MEWP distribution of the McMillin reservoir rainfall series, which is a combination of the five WP exponential distributions weighted by the central rainfall occurrence of each WP, using Eq. (1). Return periods are obtained using Eq. (2). Spatial mapping of the relative importance of each Gradex value compared to the other one for each station shows the same tendencies observed when looking for "where it rains?" for each WP (Fig. 4): the Gradex values of WP1 are close to the average value of the five Gradex values for each station, highlighting a pattern with the same relative importance over the whole domain. WP2 Gradex values are clearly the most important Gradex values for the Washington State stations, coherent information with the rainfall spatial distribution of the WP2 days (shown in Fig. 4), which are particularly rainy in this coastal area. Similarly, stations with particularly high WP3 and WP4 Gradex values compared to the other Gradex values are located in the Vancouver City area and on the Vancouver Island West Coast. Finally, WP5 Gradex values are regionally the lowest Gradex values since these days are mainly days without any observed rain. This figure highlights that the Coastal BC WP classification is useful for splitting observed precipitation series into more homogeneous sub-samples and thus identifying for each station the synoptic situations that generate the highest hazard in terms of heavy rainfall events. Thus, in this area of Coastal BC, the highest heavy rainfall hazard is mainly generated by WP2 for the major part of the Northwestern Washington region and Vancouver City region, by WP3 for the Vancouver Island region and by WP4 for the Northern Coastal BC region. Finally, an example of a MEWP probability distribution is shown with the McMillin reservoir rainfall series. This station is located in North-Western Washington State at 157 m above mean sea level. The WP

HESSD
9, 11733–11768, 2012

sub-sampling illustrated in Fig. 5b reveals five sub-populations characterised by different heavy rainfall records. WP2 thus clearly contains the heaviest rainy days of this rainfall series. Note that the final MEWP distribution illustrated in Fig. 5c fits relatively well with the heaviest observations and that the tail of the distribution is equivalent to the tail of the WP2 exponential distribution.

4.4 Link between ENSOs and Coastal BC WP frequencies

In this section, the link between El Niño Southern Oscillation anomaly and the frequency of each Coastal BC WP is analysed.

Figure 6 presents winter frequencies of the five Coastal BC WPs estimated on different year sets. First line summarises empirical winter frequency observed on the 53 Niño winters and 48 Niña winters over the 1871–2007 period (blue and red dots, respectively) while the second line summarises the empirical winter frequency observed on the 20 Niño winters and 17 Niña winters over the 1951–2001 period (blue and red dots, respectively). In order to characterise the statistical significance of the frequency change between these different year sets, bootstrap simulations were performed. A total of 1000 random combinations of, respectively, 68 and 25 winters among 136 and 50 winters were generated for each period considered. The combinations were made without consideration of the ENSO values and therefore assumed to be representative of climate variability. Frequency changes are assumed to be significant when empirical frequencies are out of the boxplots and thus could not be considered as coming from "natural" climate variability. Significant changes are mainly observed for WP2 and WP3: WP2 is more common during Niña winters rather than during Niño winters and WP3 is clearly more common during Niño winters rather than during Niña winters. Although these changes are statistically significant, the magnitudes of changes are smaller: WP2 is observed 22 % of all days during Niño winters, whereas it is observed 27 % of days during Niña winters and WP3 is observed 17 % of all days during Niña winters, whereas it is observed 22 % of days during Niño winters. Other tendencies were observed, with WP1 more common during Niña winters than during Niño winters over the 1871–2007

HESSD
9, 11733–11768, 2012

period, meaning that on average there are more rainy days throughout Coastal BC during Niña winters.

This observation is emphasised when the frequency of WPs is estimated on the "extreme ENSO winters". Table 2 shows the Coastal BC WP winter (ONDJFM) frequency of 1982–1983 and 1997–1998 Niño winters and of 1973–1974 and 1988–1989 Niña winters. These years are the most severe El Niño and La Niña years observed over the 50-yr 1951–2001 period. The frequency changes observed over all the winters are found again with these winter sub-sets, with WP2, which is clearly more common in La Niña years (32 % of all days versus 22 %) and WP3, which is clearly more common in Niño winters (37 % of all days versus 17 %). It also seems that for this set of 4 "extreme ENSO winters", WP5, which is the anticyclonic one, appears to be less common in Niño winters (15 % of all days against 8 %). This tendency is not clear when we are considering all winter sets in the Fig. 6. The most significant signal is thus a "trade-off" between WP2 and WP3 frequency of occurence.

4.5 Link between ENSOs and MEWP distributions

In this section, MEWP parameters and distributions are identified on each of the 45 rainfall series, in order to quantify the link between ENSO and MEWP parameters and MEWP distributions. First the MEWP parameters obtained over the whole set of winter precipitation records are compared with those obtained over the Niño and Niña winter sets. Second, the final MEWP distributions are compared in order to assess the impact of using different parameters on the final MEWP distributions.

Figure 7 compares the parameters of the 45 Niño MEWP distributions with the parameters of the 45 Niña MEWP distributions. It is organised as a table, with each column representing one Coastal BC WP and each line representing a parameter of the MEWP distributions. Each point represents one of the 45 rainfall series studied. Note that first two lines (λ and u) are the parameters of the exponential distribution of each WP, while the third line (p) is the mean number per year of CR events of each WP for each station. Gradex value variability using different winter sets is significant (from

−40 % to +40 %) but the impact of ENSO on this variability is not straightforward. Variability of the u parameters is slightly more limited (from −30 % to +30 %) but the ENSO impact on their values is also not clear. Nevertheless, WP1 u values seem to be significantly higher during Niña winters than during Niño winters. Finally, the variability of CR frequency for each WP is limited (from −20 % to +20 %), but ENSOs seem to significantly impact their values: WP1 and WP2 CR events are more frequent during Niña winters, while WP3 and WP4 CR events appear to be more frequent during Niño winters, as shown for WP frequency in Sect. 4.4.

The estimations of 1000-yr return period precipitation values (noted P_{1000} hereafter, exprimed in mm) were then compared. First, three MEWP distributions were defined for each of the 45 precipitation series: one considering all 50 winters, one considering 20 Niño winters and one considering 17 Niña winters and thus using the MEWP parameters illustrated in Fig. 7. A bootstrap test was then performed for each of the 45 stations in order to test the significance of eventual changes between heavy rainfall estimation over Niño winters and heavy rainfall estimation over Niña winters. Differences between these different heavy rainfall estimations were examined at the regional scale. The result of a significance test is plotted in Fig. 8, which represents the degree of significance between P_{1000} values defined on Niño winters or on Niña winters for each of the 45 stations. The colour assigned to each rainfall station represents the position of the P_{1000} values defined by MEWP distributions on Niño winters (left plot) or on Niña winters (right plot) within the distribution of 1000 values of P_{1000} values defined by MEWP distributions on a random combination of 25 winter precipitation observations. Roughly speaking, blue stations are stations where the P_{1000} values defined on Niña winters are significantly different from the total distribution and red stations are stations where P_{1000} values defined on Niño winters are significantly different from the total distribution. The number of stations where significant differences are observed is five for Niño winters and six for Niña winters, which represents, respectively, 11 % and 13 % of all stations. Note that by definition of the H0 hypothesis of the test performed, at least four stations are found as statistically different (10 % of station number). These results show that the

HESSD
9, 11733–11768, 2012

MEWP parameters for a given season and a given WP are not regionally statistically significantly influenced by ENSOs. On the other hand, the frequency of occurrence of WP and consequently the number of rainfall event observations per WP per year significantly depends on ENSOs. However, in coherence with empirical evidence on rainfall event frequency of occurrence, it is not enough to give significant trends on heavy rainfall estimation. Nevertheless, some interesting local behaviours are detected: for example, stations close to the Vancouver City area seem to be characterised by P_{1000} values greater during Niña winters and on the contrary, P_{1000} values are lower during Niño winters.

Finally, the difference between Niño and Niña winter heavy precipitation is illustrated through the McMillin reservoir precipitation series on Fig. 9a for Niño winter observations and MEWP distributions and on Fig. 9b for Niña winter observations and MEWP distributions.

5 Conclusions

A WP classification has been defined on the Coastal BC region using 177 rainfall stations and geopotential height fields over a larger area in order to analyse winter heavy rainfall events in this region. Five contrasted WPs composed this classification, four rainy WPs and one non-rainy WP, the anticyclonic pattern. The four rainy WPs are mainly observed in the winter months (October to March), which is the period of heavy precipitation events in Coastal BC and is thus consistent with the local climatology. The combination of this WP classification with the seasonal description of rainfall is shown to be useful for splitting observed precipitation series into more homogeneous sub-samples and thus identifying for each station the synoptic situations that generate the highest hazard in terms of heavy rainfall events. Thus, in this area of Coastal BC, the highest heavy rainfall hazard is mainly generated by WP2 for the major part of the North-Western Washington region and Vancouver City region, by WP3 for Vancouver Island area and by WP4 for the Northern Coastal BC region.

HESSD
9, 11733–11768, 2012

El Niño Southern Oscillations significantly influence the frequency of occurrence of two Coastal BC WPs: WP2 is more common during Niña winters rather than during Niño winters and WP3 is clearly more common during Niño winters than during Niña winters. These changes are statistically significant, but the magnitudes of changes are not great: WP2 is observed 22 % of all days during Niño winters, whereas it is observed 27 % of days during Niña winters, and WP3 is observed 17 % of all days during Niña winters, whereas it is observed 22 % of days during Niño winters. Within each WP, ENSOs seem to only influence the frequency of rainy events (MEWP parameter p) and not the magnitude of heavy rainfall events (MEWP parameters λ and u). Logically, MEWP heavy rainfall estimations do not show significant evolution of heavy rainfall behaviour between Niño and Niña winters. Finally, the WP approach allows catching the variability of the probability of occurrences of synoptic situations generating heavy rainfall depending on ENSOs. WP classification is thus useful to explain local regional patterns.

The main difference between Niño and Niña winter precipitation is thus found in the frequency of rainy events and in the mean annual amounts of precipitation, probably explaining the differences observed in the hydrological cycle (snowfall amount, flood magnitudes, etc.) previously highlighted in the literature. Thus, many "small" and "average" rainy events during a Niña winter will saturate watersheds and increase snowpack, which could produce heavy floods even from these "small" or "average" rainy events compared to a Niño winter when even a heavy rainfall storm could fall on dry soil or on below-average snowpack and result in a insignificant flood event. These hypotheses could be tested in future studies by applying methods for extreme flood estimation such as the SCHADEX method (Paquet et al., 2006) on Coastal BC catchments with the same methodology: comparing flood estimations made using all available winters with estimations made using only Niña winters, only Niño winters, and using randomly associated winter sub-sets. Future investigations could focus on other climate signals relevant for the region such as the Pacific Decadal Oscillation (PDO), an oscillation which has a significant impact on hydro-climatology in Western Canada (see Whitfield

HESSD
9, 11733–11768, 2012

et al., 2010, for a review). Combinations of different climate signals with different oscillation periods could also be important to consider.

Finally, these results open interesting perspectives in the fields of climate change prediction on heavy rainfall distribution, where WP classifications could be "medium-scale disaggregating tools" between general circulation model outputs and local rainfall observations.

Acknowledgements. Our thanks are extended to Mel Schaefer from MGS Engineering Consultants, Inc. for providing the Washington State precipitation series. Douglas McCollor and Gregory West from BC Hydro are also thanked for interesting discussions on BC WPs. This work has been done in the framework of a collaboration project between EDF and BC Hydro on comparison of flood estimation methods.

References

Allamano, P., Laio, F., and Claps, P.: Effects of disregarding seasonality on the distribution of hydrological extremes, Hydrol. Earth Syst. Sci., 15, 3207–3215, doi:10.5194/hess-15-3207-2011, 2011. 11735

Bontron, G.: Prévision quantitative des précipitations: adaptation probabiliste par recherche d'analogues. Utilisation des ré-analyses NCEP/NCAR et application aux précipitations du Sud-Est de la France, PhD thesis, Institut Polytechnique de Grenoble, 2004. 11739

Brigode, P., Bernardara, P., Gailhard, J., Garavaglia, F., Ribstein, P., and Merz, R.: Optimization of the geopotential heights information used in a rainfall-based weather patterns classification over Austria, Int. J. Climatol., doi:10.1002/joc.3535, in press, 2012. 11738, 11739

Casola, J. H. and Wallace, J. M.: Identifying weather regimes in the wintertime 500 hPa geopotential height field for the Pacific–North American sector using a limited-contour clustering technique, J. Appl. Meteorol. Clim., 46, 1619–1630, doi:10.1175/JAM2564.1, 2007. 11735, 11742

Cayan, D. R., Redmond, K. T., and Riddle, L. G.: ENSO and hydrologic extremes in the Western United States, J. Climate, 12, 2881–2893, doi:10.1175/1520-0442(1999)012<881:EAHEIT>2.0.CO;2, 1999. 11736

Chen, W. Y. and van den Dool, H. M.: Significant change of extratropical natural variability and potential predictability associated with the El Niño/Southern Oscillation, Tellus A, 51, 790–802, doi:10.1034/j.1600-0870.1999.00017.x, 1999. 11735

Cheng, X. and Wallace, J. M.: Cluster analysis of the Northern Hemisphere wintertime 500 hPa height field: spatial patterns, J. Atmos. Sci., 50, 2674–2696, doi:10.1175/1520-0469(1993)050<2674:CAOTNH>2.0.CO;2, 1993. 11738

Coles, S., Pericchi, L. R., and Sisson, S.: A fully probabilistic approach to extreme rainfall modeling, J. Hydrol., 273, 35–50, doi:10.1016/S0022-1694(02)00353-0, 11735

Compo, G. P., Whitaker, J. S., Sardeshmukh, P. D., Matsui, N., Allan, R. J., Yin, X., Gleason, B. E., Vose, R. S., Rutledge, G., Bessemoulin, P., Brönnimann, S., Brunet, M., Crouthamel, R. I., Grant, A. N., Groisman, P. Y., Jones, P. D., Kruk, M. C., Kruger, A. C., Marshall, G. J., Maugeri, M., Mok, H. Y., Nordli, Ø., Ross, T. F., Trigo, R. M., Wang, X. L., Woodruff, S. D., and Worley, S. J.: The twentieth century reanalysis project, Q. J. Roy. Meteorol. Soc., 137, 1–28, doi:10.1002/qj.776, 2011. 11743

Dettinger, M.: Fifty-two years of "pineapple-express" Storms across the West Coast of North America, Tech. Rep. CEC-500-2005-004, US Geological Survey, Scripps Institution of Oceanography for the California Energy Commission, PIER Energy-Related Environmental Research, La Jolla, California, 2004. 11737

Djerboua, A. and Lang, M.: Scale parameter of maximal rainfall distribution: comparison of three sampling techniques, Revue des Sciences de l'Eau, 20, 111–125, doi:10.7202/015740ar, 2007. 11735

Ducić, V., Luković, J., Burić, D., Stanojević, G., and Mustafić, S.: Precipitation extremes in the wettest Mediterranean region (Krivošije) and associated atmospheric circulation types, Nat. Hazards Earth Syst. Sci., 12, 687–697, doi:10.5194/nhess-12-687-2012, 2012. 11735

Feldl, N. and Roe, G. H.: Climate variability and the shape of daily precipitation: a case study of ENSO and the American West, J. Climate, 24, 2483–2499, doi:10.1175/2010JCLI3555.1, 2011. 11736

Fernández-González, S., del Río, S., Castro, A., Penas, A., Fernández-Raga, M., Calvo, A. I., and Fraile, R.: Connection between NAO, weather types and precipitation in León, Spain (1948–2008), Int. J. Climatol., doi:10.1002/joc.2431, in press, 2011. 11735

Fréchet, M.: Sur la loi de probabilité de l'écart maximum, Annales de la Société Polonaise de Mathématiques, 6, 92–116, 1927. 11735

Garavaglia, F., Gailhard, J., Paquet, E., Lang, M., Garçon, R., and Bernardara, P.: Introducing a rainfall compound distribution model based on weather patterns sub-sampling, Hydrol. Earth Syst. Sci., 14, 951–964, doi:10.5194/hess-14-951-2010, 2010. 11735, 11737, 11738, 11739, 11740

Garavaglia, F., Lang, M., Paquet, E., Gailhard, J., Garçon, R., and Renard, B.: Reliability and robustness of rainfall compound distribution model based on weather pattern sub-sampling, Hydrol. Earth Syst. Sci., 15, 519–532, doi:10.5194/hess-15-519-2011, 2011. 11735

Gershunov, A.: ENSO influence on intraseasonal extreme rainfall and temperature frequencies in the contiguous United States: implications for long-range predictability, J. Climate, 11, 3192–3203, doi:10.1175/1520-0442(1998)011<3192:EIOIER>2.0.CO;2, 1998. 11736

Guilbaud, S. and Obled, C.: Daily quantitative precipitation forecast by an analogue technique: optimisation of the analogy criterion, Compte Rendus de l'Académie des Sciences – Séries IIA – Earth and Planetary Science, 327, 181–188, doi:10.1016/S1251-8050(98)80006-2, 1998. 11739

Gumbel, E. J.: Statistics of Extremes, Columbia University Press, New York, 1958. 11735

Higgins, R., Schemm, J., Shi, W., and Leetmaa, A.: Extreme precipitation events in the Western United States related to tropical forcing, J. Climate, 13, 793–820, 2000. 11736

Kenyon, J. and Hegerl, G. C.: Influence of modes of climate variability on global precipitation extremes, J. Climate, 23, 6248–6262, doi:10.1175/2010JCLI3617.1, 2010. 11736

Kimoto, M. and Ghil, M.: Multiple flow regimes in the Northern Hemisphere winter, Pt. II: sectorial regimes and preferred transitions, J. Atmos. Sci., 50, 2645–2673, 1993. 11735

Mass, C., Skalenakis, A., and Warner, M.: Extreme precipitation over the West Coast of North America: is there a trend?, J. Hydrometeorol., 12, 310–318, doi:10.1175/2010JHM1341.1, 2011. 11737

McCabe, G. and Muller, R.: Effects of ENSO on weather-type frequencies and properties at New Orleans, Louisiana, USA, Clim. Res., 20, 95–105, 2002. 11735

Neiman, P. J., Schick, L. J., Ralph, F. M., Hughes, M., and Wick, G. A.: Flooding in Western Washington: the connection to atmospheric rivers, J. Hydrometeorol., 12, 1337–1358, doi:10.1175/2011JHM1358.1, 2011. 11737

Obled, C., Bontron, G., and Garçon, R.: Quantitative precipitation forecasts: a statistical adaptation of model outputs through an analogues sorting approach, Atmos. Res., 63, 303–324, doi:10.1016/S0169-8095(02)00038-8, 2002. 11739, 11740

HESSD
9, 11733–11768, 2012

Pague, B. S. and Blandford, S. M.: Weather types, in: Weather Forecasting and Weather Types on the North Pacific Slope, Weather Bureau Print, Portland, Oregon, 20–29, 1897. 11735

Paquet, E., Gailhard, J., and Garçon, R.: Evolution of the GRADEX method: improvement by atmospheric circulation classification and hydrological modelling, La Houille Blanche, 5, 80–90, doi:10.1051/lhb:2006091, 2006. 11752

Pickands, J. P.: Statistical Inference using extreme order statistics, Ann. Stat., 3, 119–131, doi:10.1214/aos/1176343003, 1975. 11735

Robertson, A. W. and Ghil, M.: Large-scale weather regimes and local climate over the Western United States, J. Climate, 12, 1796–1813, doi:10.1175/1520-0442(1999)012<1796:LSWRAL>2.0.CO;2, 1999. 11735

Schubert, S. D., Chang, Y., Suarez, M. J., and Pegion, P. J.: ENSO and wintertime extreme precipitation events over the contiguous United States, J. Climate, 21, 22–39, doi:10.1175/2007JCLI1705.1, 2008. 11735

Shabbar, A., Bonsal, B., and Khandekar, M.: Canadian precipitation patterns associated with the southern oscillation, J. Climate, 10, 3016–3027, doi:10.1175/1520-0442(1997)010<3016:CPPAWT>2.0.CO;2, 1997. 11736

Sheridan, S. C.: The redevelopment of a weather-type classification scheme for North America, Int. J. Climatol., 22, 51–68, doi:10.1002/joc.709, 2002. 11735

Stahl, K., Moore, R. D., and Mckendry, I. G.: The role of synoptic-scale circulation in the linkage between large-scale ocean–atmosphere indices and winter surface climate in British Columbia, Canada, Int. J. Climatol., 26, 541–560, doi:10.1002/joc.1268, 2006. 11735

Teweles, J. and Wobus, H.: Verification of prognosis charts, B. Am. Meteorol. Soc., 35, 455–463, 1954. 11740

Trenberth, K.: The definition of El Niño, B. Am. Meteorol. Soc., 78, 2771–2778, 1997. 11741, 11744

Ward, J. H.: Hierarchical grouping to optimize an objective function, J. Am. Stat. Assoc., 58, 236–244, doi:10.2307/2282967, 1963. 11738

Whitfield, P. H., Moore, R. D., Fleming, S. W., and Zawadzki, A.: Pacific decadal oscillation and the hydroclimatology of Western Canada – review and prospects, Can. Wat. Resour. J., 35, 1–28, doi:10.4296/cwrj3501001, 2010. 11752

Yarnal, B. and Diaz, H. F.: Relationships between extremes of the southern oscillation and the winter climate of the Anglo-American Pacific Coast, J. Climatol., 6, 197–219, doi:10.1002/joc.3370060208, 1986. 11736

Zhang, X., Wang, J., Zwiers, F. W., and Groisman, P. Y.: The influence of large-scale climate variability on winter maximum daily precipitation over North America, J. Climate, 23, 2902–2915, doi:10.1175/2010JCLI3249.1, 2010. 11736

HESSD
9, 11733–11768, 2012

Linking ENSO and heavy rainfall events over Coastal British Columbia

P. Brigode et al.

Table 1. Yearly and seasonal frequencies of the five Coastal BC WP for 1871–2007, 1951–2001 and 1983–2003 periods.

	1871–2007			1951–2001			1983–2003		
	Year	ONDJFM	AMJJAS	Year	ONDJFM	AMJJAS	Year	ONDJFM	AMJJAS
WP1	11 %	11 %	10 %	10 %	9 %	10 %	9 %	7 %	10 %
WP2	14 %	23 %	5 %	15 %	24 %	6 %	15 %	23 %	7 %
WP3	15 %	20 %	10 %	16 %	19 %	12 %	17 %	21 %	13 %
WP4	25 %	33 %	17 %	28 %	36 %	19 %	27 %	36 %	19 %
WP5	35 %	12 %	58 %	32 %	12 %	53 %	32 %	12 %	51 %

HESSD
9, 11733–11768, 2012

Title Page
Abstract | Introduction
Conclusions | References
Tables | Figures
◀| |▶
◀ ▶
Back | Close
Full Screen / Esc
Printer-friendly Version
Interactive Discussion

Table 2. Average Coastal BC WP winter (ONDJFM) frequency of 1982–1983 and 1997–1998 Niño winters and of 1973–1974 and 1988–1989 la Niña winters.

ENSO Winters	WP1	WP2	WP3	WP4	WP5
1982–1983 and 1997–1998 El Niño winters	9 %	22 %	37 %	24 %	8 %
1973–1974 and 1988–1989 La Niña winters	10 %	32 %	17 %	26 %	15 %

HESSD
9, 11733–11768, 2012
Linking ENSO and heavy rainfall events over Coastal British Columbia
P. Brigode et al.

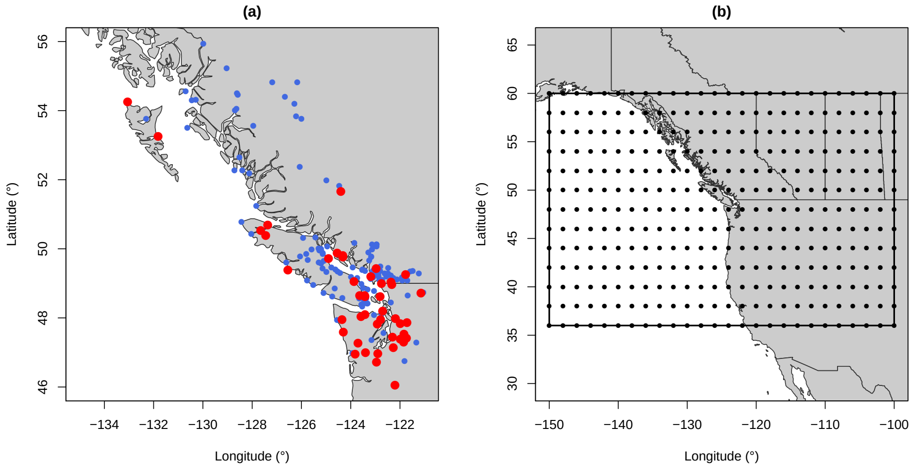

Fig. 1. (a) Location of the 177 rainfall series used for the Coastal BC WP definition (blue dots) and the 45 rainfall series used for the quantification of the influence of ENSO on rainfall characteristics (red dots). **(b)** Location of the 338 geopotential grid points used for the Coastal BC WP definition.

HESSD
9, 11733–11768, 2012

Linking ENSO and heavy rainfall events over Coastal British Columbia

P. Brigode et al.

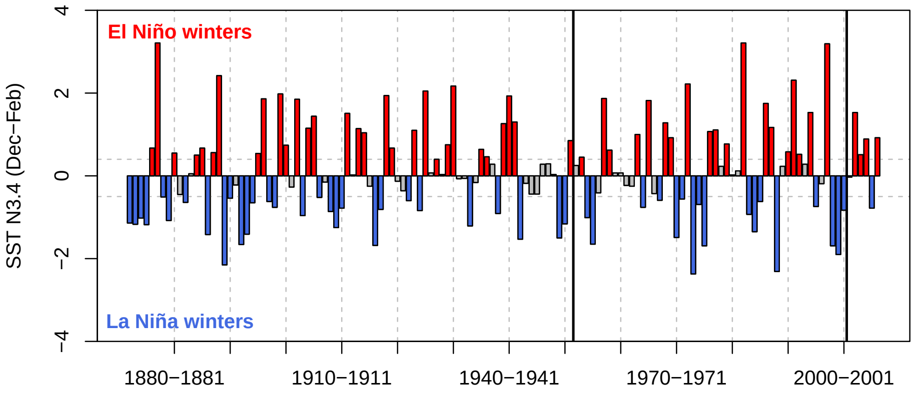

Fig. 2. Classification of 1872–2007 winters (ONDJFM) using SST Niño 3.4 Index, resulting in La Niña winters (blue color), neutral winters (grey color) and El Niño winters (red color). The 1951–2001 period (the period used for quantification of the influence of ENSO on rainfall characteristics) is highlighted by black vertical lines.

HESSD
9, 11733–11768, 2012

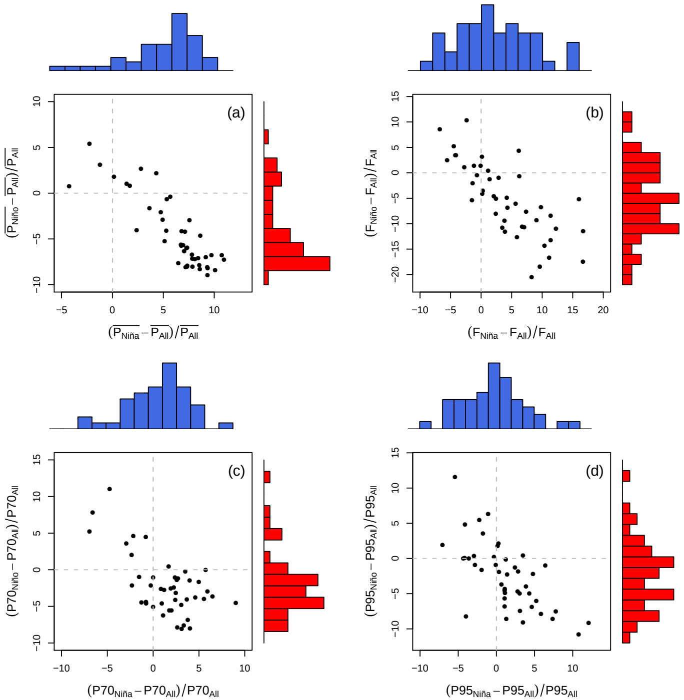

Fig. 3. Relative difference between rainfall characteristics of the whole record periods (50 winters) and over the Niña winters (17 winters) and relative difference between rainfall characteristics of the whole record periods (50 winters) and over the Niño winters (20 winters) for each station considered and for four rainfall characteristics: **(a)** the average of winter precipitation values, **(b)** frequency of the days when more than 20 mm were observed, **(c)** 0.70 percentile and **(d)** 0.95 percentile of the rainfall distributions. Blue (Niña winters) and red (Niño winters) histograms represent for each of the four graphs the distributions of the (x) and the (y) axis values.

HESSD

9, 11733–11768, 2012

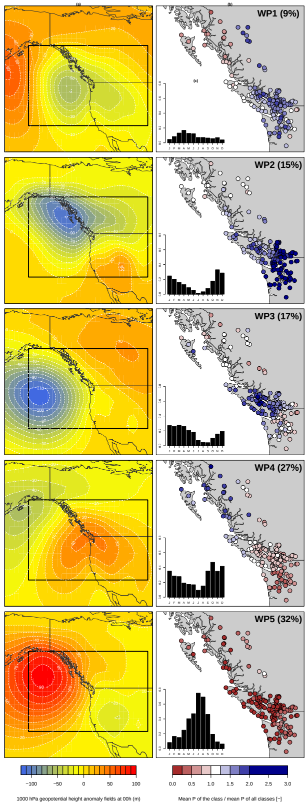

Fig. 4. Geopotential height anomaly fields (1000 hPa at 0 h) and station ratio between the mean precipitation amount and the general precipitation (considering all weather patterns) for each of the five Coastal BC WPs. Black boxes indicate the spatial coverage of the geopotential space used.

HESSD
9, 11733–11768, 2012

Linking ENSO and heavy rainfall events over Coastal British Columbia

P. Brigode et al.

HESSD
9, 11733–11768, 2012

Linking ENSO and heavy rainfall events over Coastal British Columbia

P. Brigode et al.

Title Page
Abstract | Introduction
Conclusions | References
Tables | Figures
◀I | ▶I
◀ | ▶
Back | Close
Full Screen / Esc
Printer-friendly Version
Interactive Discussion

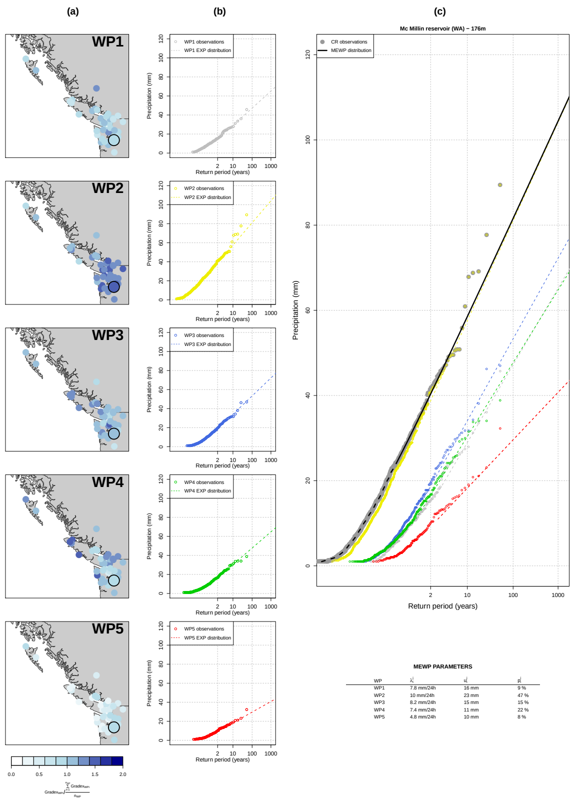

WP	λ_i^j	u_i^j	p_i^j
WP1	7.8 mm/24h	16 mm	9 %
WP2	10 mm/24h	23 mm	47 %
WP3	8.2 mm/24h	15 mm	15 %
WP4	7.4 mm/24h	11 mm	22 %
WP5	4.8 mm/24h	10 mm	8 %

Fig. 5. (a) Ratios estimated for 45 rainfall stations and each Coastal BC WP between the Gradex value of the WP considered (parameter λ) and the average value of the five Gradex values for the station considered. The McMillin reservoir rainfall series is highlighted with a black circle. **(b)** Comparison between the whole CR distribution of the McMillin reservoir rainfall series and CR sub-samples of the five Coastal BC WPs. **(c)** MEWP distribution of the winter season (ONDJFM) of the 1951–2001 period for the McMillin reservoir rainfall series.

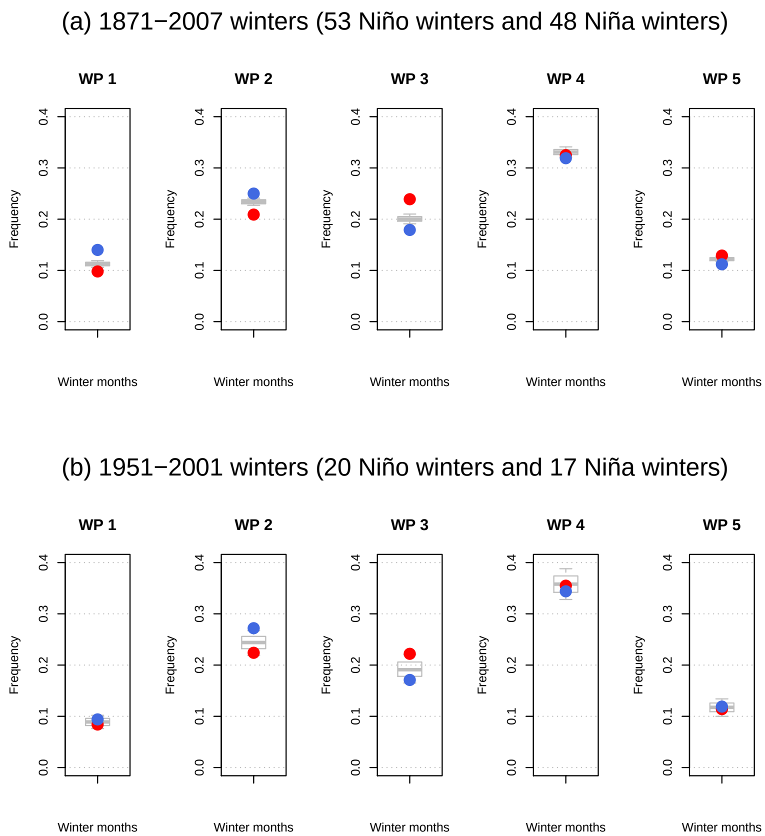

Fig. 6. Winter frequency of the five Coastal BC WPs estimated on Niño and Niña winters over **(a)** the 1871–2007 period and over **(b)** the 1951–2001 period; compared with 1000 random combinations of 68 winters out of 136 and 25 winters out of 50 for the 1871–2007 and the 1951–2001 periods, respectively, produced by bootstrap simulations. The boxplots show the 0.10, 0.25, 0.50, 0.75 and 0.90 percentiles.

HESSD
9, 11733–11768, 2012

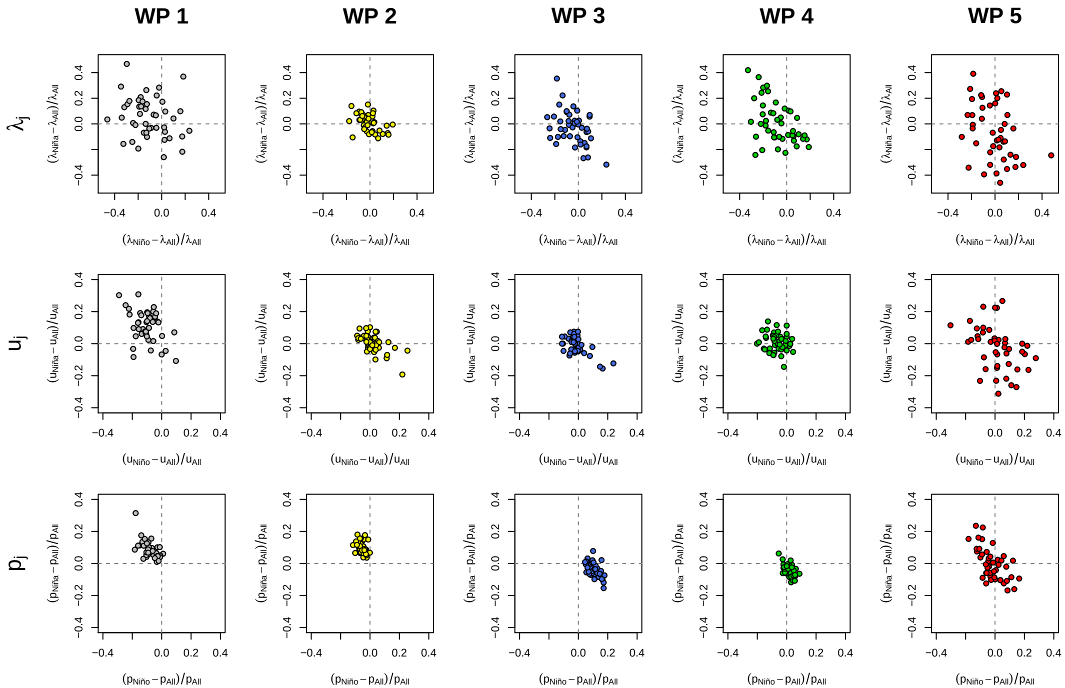

Fig. 7. Comparison of the MEWP distribution parameters obtained on 20 Niño winters and 17 Niña winters defined on the 45 stations for each of the five Coastal BC WPs.

HESSD
9, 11733–11768, 2012

Linking ENSO and heavy rainfall events over Coastal British Columbia

P. Brigode et al.

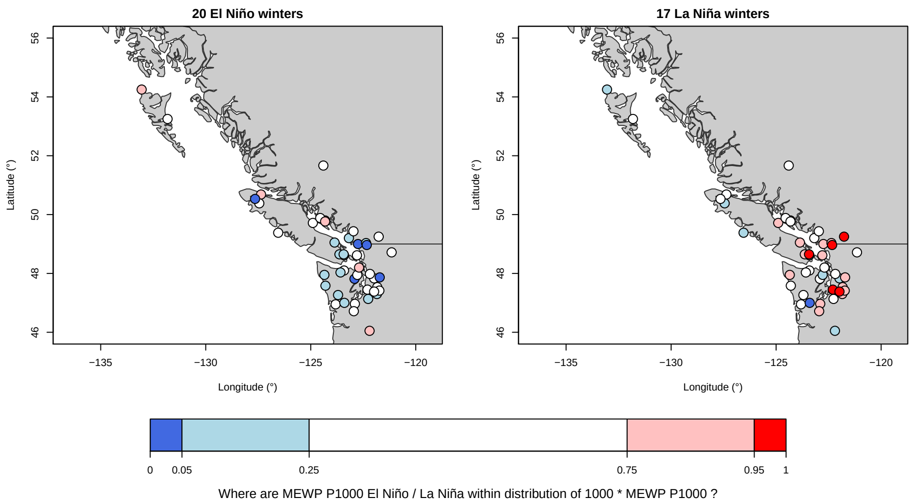

Fig. 8. Degree of significance between P_{1000} values estimated by MEWP distributions defined over 20 Niño winters or on 17 Niña winters for each of the 45 stations and P_{1000} values estimated by MEWP distributions defined over random combination of 25 winter precipitation observations generated by bootstrap simulations.

HESSD
9, 11733–11768, 2012

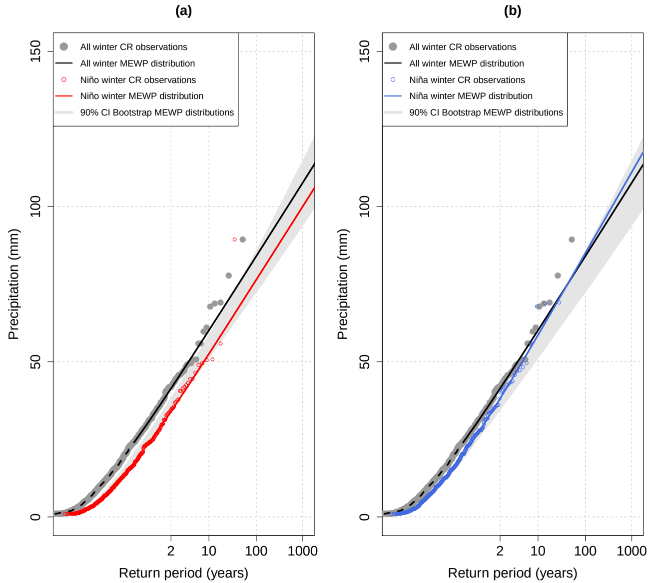

MEWP PARAMETERS (a)

WP	λ_i^j	u_i^j	p_i^j
WP1	4.5 mm/24h	12 mm	9 %
WP2	10.3 mm/24h	23 mm	43 %
WP3	6.2 mm/24h	13 mm	19 %
WP4	6.3 mm/24h	10 mm	22 %
WP5	3.8 mm/24h	12 mm	7 %
WP1	7.9 mm/24h	15 mm	9 %
WP2	10.3 mm/24h	23 mm	45 %
WP3	8 mm/24h	15 mm	14 %
WP4	7 mm/24h	10 mm	21 %
WP5	5 mm/24h	11 mm	10 %

MEWP PARAMETERS (b)

WP	λ_i^j	u_i^j	p_i^j
WP1	7.8 mm/24h	17 mm	10 %
WP2	11.4 mm/24h	23 mm	50 %
WP3	6.9 mm/24h	17 mm	12 %
WP4	6.5 mm/24h	10 mm	21 %
WP5	6 mm/24h	12 mm	7 %
WP1	7.9 mm/24h	15 mm	9 %
WP2	10.3 mm/24h	23 mm	45 %
WP3	8 mm/24h	15 mm	14 %
WP4	7 mm/24h	10 mm	21 %
WP5	5 mm/24h	11 mm	10 %

Fig. 9. MEWP distributions for the winter season (ONDJFM) defined over the 1951–2001 period, Niño winters, Niña winters and 1000 random combinations of 25 winters for the McMillin reservoir rainfall series.

HESSD
9, 11733–11768, 2012

Linking ENSO and heavy rainfall events over Coastal British Columbia

P. Brigode et al.